Natural Resources Research, Vol. 30, No. 3, June 2021 (© 2021)
https://doi.org/10.1007/s11053-021-09847-z

Original Paper

Determination of In Situ Wettability Using Wavelet Analysis and Nuclear Magnetic Resonance Log Data

Mohammad Heidary [1,2]

Received 22 December 2020; accepted 13 February 2021
Published online: 2 March 2021

Knowledge of reservoir rock wettability is crucial for the understanding of fluid displacement mechanisms and for adopting feasible solutions to enhance oil recovery. Highly sensitive to the strength of fluid–rock interactions, nuclear magnetic resonance (NMR) measurements are a well-suited candidate for in situ wettability determination. Changes in correlation coefficients between NMR porosity (ϕ_{NMR}) and transverse relaxation time (T_2) can be used as a diagnostic parameter to determine in situ wettability. This paper aimed to take advantage of this promising feature to specify the downhole wettability of an oil well running through two carbonate reservoirs. In this regard, the correlation coefficient between ϕ_{NMR} and T_2 was first computed at each depth. As a superior technique in analyzing non-stationary signals, the wavelet transform was then applied to the correlation coefficient log to remove shale content. Finally, the wavelet transform was re-applied to the modified correlation coefficient log to derive the detail coefficients. Scrutiny of the detail coefficients revealed a strong correlation with experimental wettability results. The results obtained from this investigation indicated that positive detail coefficients are associated with water-wet, and negative ones with oil-wet media.

KEY WORDS: Wettability, Nuclear magnetic resonance, Transverse relaxation time, Wavelet transform.

INTRODUCTION

Wettability is one of the fundamental parameters governing multiphase flow through porous media. Reservoir rock wettability significantly influences transport characteristics, such as irreducible saturation, relative permeability, and capillary pressure. There are various laboratory techniques for extracting meaningful wettability information from rock core plugs, such as the U.S. Bureau of Mines (USBM) test and the Amott–Harvey test. Not only are these techniques costly and time-consuming, but they also only grant information on a small scale. Moreover, these techniques require core samples to be retrieved from boreholes and analyzed in the laboratory. Therefore, the development of a technique for evaluating in situ wettability is essential. Among the most ambitious efforts to develop such a technique is nuclear magnetic resonance (NMR). Inherently responsive to the strength of fluid–rock interactions, NMR measurements provide a viable framework for determining in situ wettability. This paper attempted to determine the downhole wettability of an oil well running through two carbonate reservoirs based on the NMR relaxation property. NMR relaxation is highly sensitive to the wetting state of rock through the influence of surface relaxivity.

The state-of-the-art NMR technique has emerged over the last few decades as a relatively

[1]Research Institute of Petroleum Industry (RIPI), Tehran, Iran.
[2]To whom correspondence should be addressed; e-mail: heidarym@hotmail.com

simple and powerful tool for characterizing reservoir rock wettability. Wettability affects the three main NMR parameters, namely longitudinal relaxation time (T_1), transverse relaxation time (T_2), and diffusivity (D). Generally, the NMR-based methods proposed in the literature to quantify downhole wettability include T_2 spectrum (or T_2 shift), restricted diffusion (or $D - T_2$ map), and $\frac{T_1}{T_2}$ ratio. In the T_2 spectrum method, a forward model is first constructed based on different parameters that affect T_2. The forward model is then inverted with a numerical method to determine the wettability and saturation functions (Al-Muthana et al. 2016; Cheng et al. 2017; Dick et al. 2019; Looyestijn & Hofman, 2006; Sauerer et al. 2019). Extracting the reliable and quantitative wettability information from T_2 spectrum measurements requires a few extra pieces of information. This information is available only from the laboratory. The downhole application of this method is usually qualitative. In the restricted diffusion method, diffusivity is first measured accurately for all relaxation times. Then, the location of water and oil is determined visually on the $D - T_2$ map. Finally, by fitting the restricted diffusion lines to the fluid signals, the wettability type is determined (Liang et al. 2019a, b; Minh et al. 2015; Wang et al. 2019). Using the ratio between the two relaxation parameters T_1 and T_2 $\left(\frac{T_1}{T_2}\right)$ is a well-established method for determining downhole wettability (Katika et al. 2016; Korb et al. 2018; Valori et al. 2017). Despite being strongly correlated with the industry wettability index, this method has some disadvantages, including time-consuming measurements of T_1 relative to T_2, and achieving only a single point on the T_1 polarization curve compared to multiple points on the T_2 decay for each scan.

Given the limitations of the NMR-based methods presented for determining downhole wettability, this study intended to develop a rigorous method based on the correlation between T_2 and NMR porosity (ϕ_{NMR}). Variation in correlation coefficient between T_2 and ϕ_{NMR} was assumed to be associated with wettability. Wavelet transform, as an information processing technique, was utilized to exhibit the variation and substantiate this hypothesis. Recently, wavelet analysis has contributed remarkably to researchers in the broad field of earth science, such as geophysics, petroleum engineering, and geology. In geophysical studies, wavelet transforms have been applied to furnish high-resolution information (Grasseau et al. 2019; Yue et al. 2019) and to detect fault systems (Saadatinejad & Sarkarinejad, 2011; Xu & Sun, 2014). Outstanding results of using the wavelet transform have been reported in reservoir and geology studies by Awotunde and Horne (2013), Rezapour et al. (2019), Heidary and Fouladi Hossein Abad (2020), and Azamipour et al. (2020). Several investigations have corroborated the advantage of wavelet transform in denoising NMR log data (Ge et al. 2015; Heidary et al. 2019; Wu et al. 2012; Xie et al. 2014).

This study intended to determine the in situ wettability of reservoir rocks based on the discrete wavelet transform (DWT) of NMR log data. Generally, the steps involved in this work are as follows: provide a correlation function to calculate the correlation coefficient between T_2 and ϕ_{NMR} at each depth; apply the DWT to the correlation coefficients to remove the shale effect, if any, decompose the modified correlation coefficients to extract its details, and establish a relationship between details and Amott–Harvey wettability index.

MATERIALS AND METHODS

This study focused on determining the in situ wettability of an oil well running through two argillaceous limestone reservoirs (A and B). These reservoirs are located in the northwest of the Persian Gulf. In both reservoirs, the NMR and conventional logs were recorded. The special core analysis test and the Amott–Harvey wettability test were conducted for reservoir A. For reservoir B, there was a limited wettability test. Tables 1 and 2 display the results of the Amott–Harvey wettability test in reservoirs A and B, respectively. Figure 1a and b shows the gamma-ray (GR) log in reservoirs A and B, respectively. Figures 2 and 3 show the ϕ_{NMR} and T_2 logs for reservoirs A and B, respectively. The procedure used to determine the in situ wettability of reservoir rocks through wavelet analysis of NMR log data is as follows.

1. The correlation coefficient between T_2 and ϕ_{NMR} was computed at each depth using an appropriate correlation function, thereby achieving a correlation coefficient log.
2. The DWT was employed to remove the shale effect, if any, from the correlation coefficient log. The resulting log was referred to as a decorrelated coefficient log.

Table 1. Amott–Harvey wettability test indices for reservoir A

Depth (m)	Water wettability Index (I_W)	Oil wettability index (I_O)	Amott–Harvey index ($I_{W-O} = I_W - I_O$)	Wettability
2212.8–2213.2	0.080	0.060	0.020	Neutral
2225.7–2226.1	0.070	0.600	− 0.53	Oil-wet
2227.6–2228.0	0.540	0.001	0.539	Water-wet
2232.2–2232.6	0.250	0.080	0.170	Water-wet
2234.3–2234.7	0.380	0.001	0.379	Water-wet
2238.3–2238.7	0.519	0.288	0.231	Water-wet
2241.0–2241.4	0.422	0.542	− 0.12	Oil-wet
2241.5–2241.9	0.303	0.410	− 0.107	Oil-wet
2242.3–2242.7	0.450	0.092	0.358	Water-wet
2247.6–2248.0	0.049	0.120	− 0.071	Oil-wet
2249.5–2249.9	0.037	0.780	− 0.743	Oil-wet
2264.0–2264.4	0.960	0.001	0.959	Water-wet
2266.0–2266.4	0.756	0.001	0.755	Water-wet
2269.5–2269.9	0.530	0.013	0.517	Water-wet

Table 2. Amott–Harvey wettability test indices for reservoir B

Depth (m)	Water wettability Index (I_W)	Oil wettability index (I_O)	Amott–Harvey index ($I_{W-O} = I_W - I_O$)	Wettability
2078.2–2078.6	0.042	0.032	0.012	Neutral
2100.0–2100.4	0.381	0.001	0.380	Water-wet
2112.2–2112.6	0.031	0.763	− 0.732	Oil-wet

3. The DWT was re-employed to decompose the decorrelated coefficient log in reservoir A and extract its detail coefficients.
4. The relationship between detail coefficients and the Amott–Harvey wettability index was investigated for reservoir A. The result obtained was then extended to reservoir B.

Characterizing Wettability with Nuclear Magnetic Resonance

Nuclear magnetic resonance (NMR) refers to the response of atomic nuclei to magnetic fields. The first step in making an NMR measurement is to align, or polarize, nuclear spin axes with a static magnetic field. The second step in the NMR measurement cycle is to tip the magnetization from the longitudinal direction to a transverse plane. This tipping is performed by applying an oscillating magnetic field perpendicular to the static magnetic field. The properties of the pore space and the fluids inside are associated with transverse magnetization, which is an exponential decay process. In a uniform magnetic field, the transverse magnetization at time t, $M(t)$, is given by Coates et al. (1999):

$$M(t) = M_0 \exp\left(-\frac{t}{T_2}\right), \tag{1}$$

where M_0 is the total initial magnetization at time $t = 0$; it is calibrated to give porosity (ϕ_{NMR}). NMR measurements are affected by wettability because the pore surface promotes the relaxation rate of the wetting fluid. When a nonwetting phase becomes partially wetting, T_2 decreases dramatically because of the surface relaxation mechanism coming into play. Put differently, T_2 in the porous medium is dominated by the surface relaxation rate. The rate of surface relaxation is proportional to pore size (Dunn et al. 2002). Accordingly, the correlation between T_2 and ϕ_{NMR} can be used as a diagnostic parameter to distinguish wettability types. The calculation of the correlation coefficient between T_2 and ϕ_{NMR} at each depth entails providing an appropriate correlation function. The linear correlation coefficient (R) between T_2 and ϕ_{NMR} is calculated as (Hayter, 2012):

$$R = \frac{\sum_{z=1}^{n}\left(T_2(z) - \overline{T_2}\right)\left(\phi_{\mathrm{NMR}}(z) - \overline{\phi_{\mathrm{NMR}}}\right)}{\sqrt{\sum_{z=1}^{n}\left(T_2(z) - \overline{T_2}\right)^2\left(\phi_{\mathrm{NMR}}(z) - \overline{\phi_{\mathrm{NMR}}}\right)^2}}, \tag{2}$$

where $\overline{T_2}$ and $\overline{\phi_{\mathrm{NMR}}}$ are the averages of T_2 and ϕ_{NMR}, respectively.

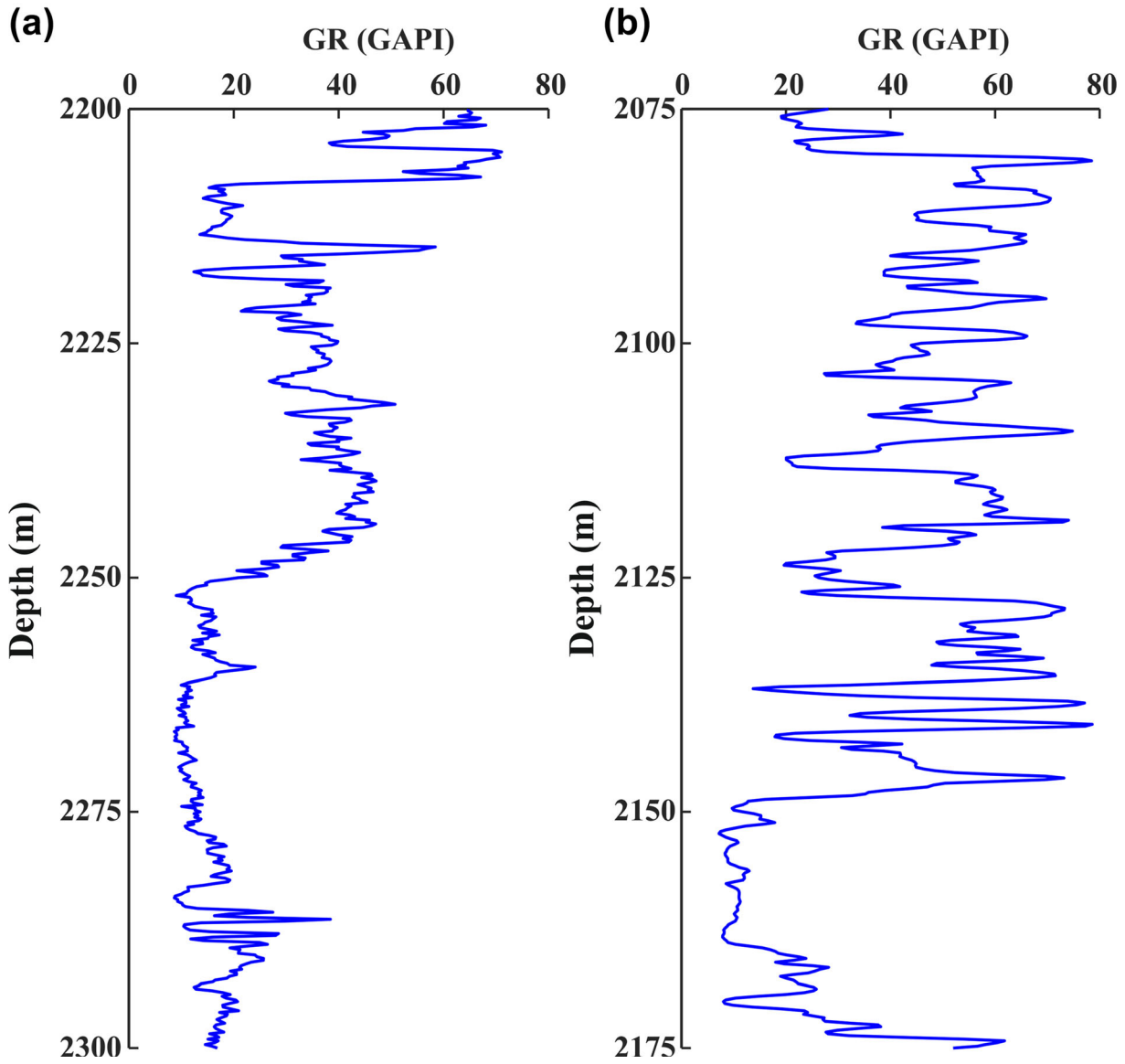

Figure 1. GR log: **a** reservoir A; **b** reservoir B.

Discrete Wavelet Transform

The discrete wavelet transform (DWT) is applied to extract features and obtain information from any given signal. The practical design of the DWT is rooted in the multiresolution analysis (MRA), which entails decomposing the function space into a coarse approximation space. Assuming that $\{V_j\}_{j\in Z}$ is a MRA of $L^2(R)$, the subspaces V_j are nested in the following manner (Jansen & Oonincx, 2005):

$$V_j \subset V_{j+1} \quad \text{and} \quad V_{j+1} = V_j \otimes W_j, \tag{3}$$

where j denotes the level (or scale) of decomposition, and the subspace W_j is the orthogonal complement of V_j in V_{j+1}. The subspaces V_j and W_j can be generated through dilations (j) and translations (k) of the scaling $\phi(t)$ and wavelet $\psi(t)$ functions, thus:

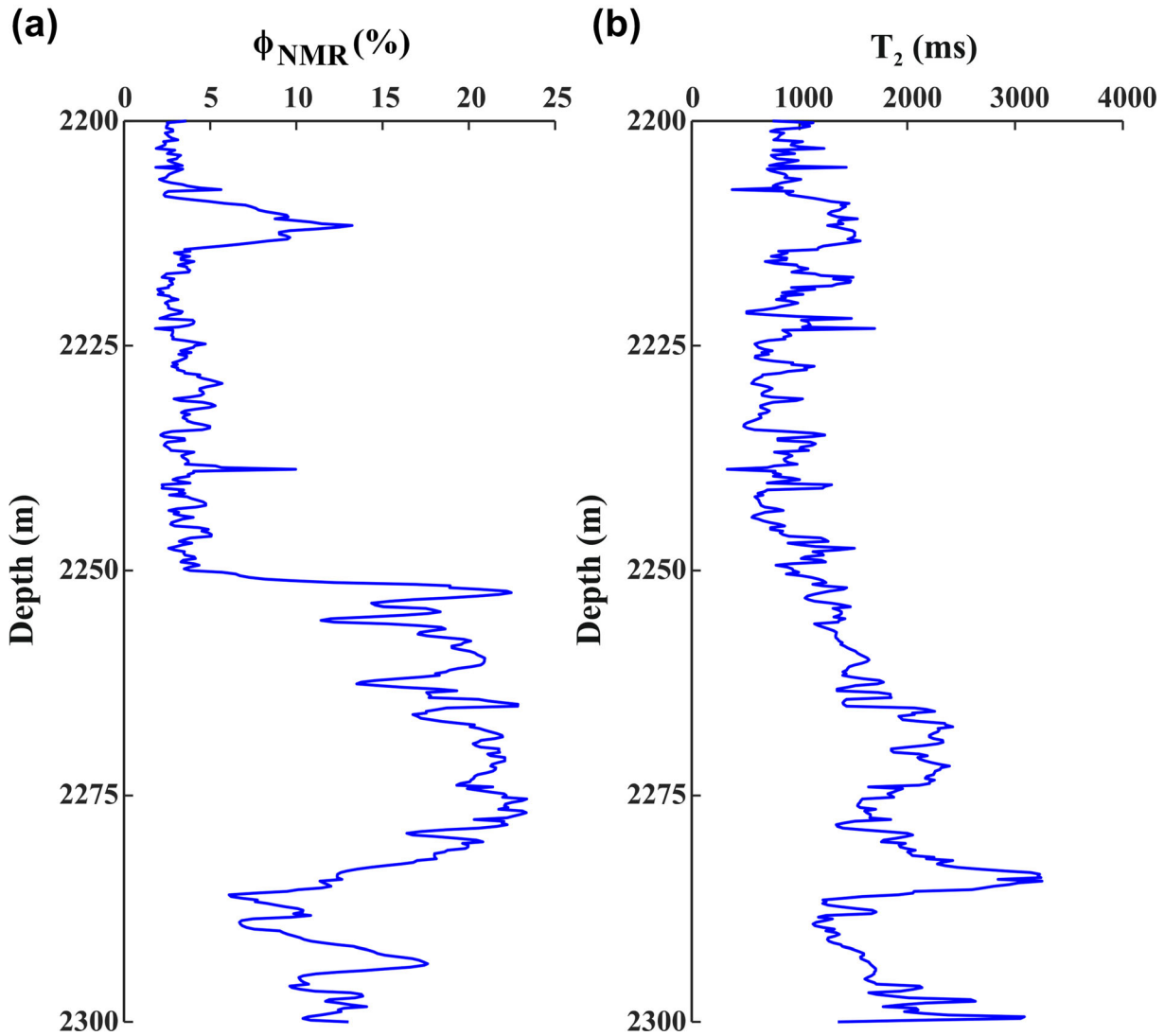

Figure 2. Logs in reservoir A: **a** ϕ_{NMR}; **b** T_2.

$$V_j = \overline{span\left\{\phi_{j.k}(t)\right\}}, \quad \text{where} \quad \phi_{j.k}(t) = 2^{\frac{j}{2}}\phi\left(2^j t - k\right) \tag{4}$$

$$W_j = \overline{span\left\{\psi_{j.k}(t)\right\}}, \quad \text{where} \quad \psi_{j.k}(t) = 2^{\frac{j}{2}}\psi\left(2^j t - k\right) \tag{5}$$

Repeating recursively the decomposition of V_j into the direct sum of a sequence of wavelet spaces yields:

$$V_j = V_0 \overset{j-1}{\underset{l=0}{\oplus}} W_l \tag{6}$$

As a result, any function $f(t) \in L^2(R)$ can be expanded as:

$$f(t) = \sum_{k\in Z} c_{j.k}\phi_{j.k}(t) + \sum_{j\geq 0}\sum_{k\in Z} d_{j.k}\psi_{j.k}(t), \tag{7}$$

where $c_{j.k}$ is coarse (approximation) coefficients and $d_{j.k}$ is wavelet (detail) coefficients. The coarse and wavelet coefficients are calculated as:

$$c_{j\cdot k} = f(t)\cdot\phi_k(t), \quad d_{j\cdot k} = f(t)\cdot\psi_{j\cdot k}(t). \tag{8}$$

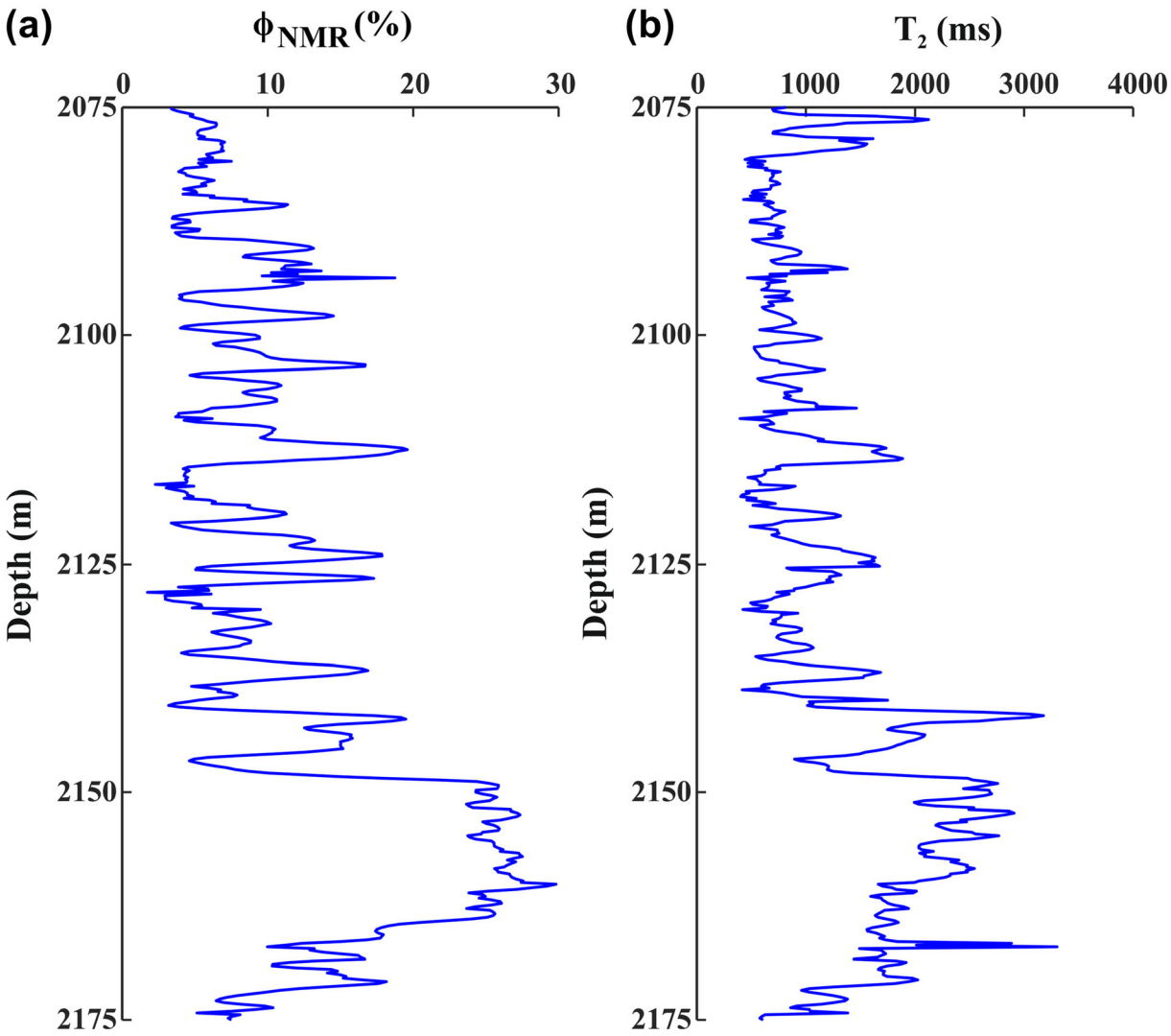

Figure 3. Logs in reservoir B: **a** ϕ_{NMR}; **b** T_2.

RESULTS AND DISCUSSION

Correlation Coefficient Log

In the oil reservoirs under study, T_2 exhibited a linear correlation with ϕ_{NMR}. The values of R between T_2 and ϕ_{NMR} in reservoirs A and B were 0.68 and 0.79, respectively. Accordingly, the correlation coefficient between T_2 and ϕ_{NMR} can be calculated at each depth using Eq. 2. For this purpose, an interval equal to the core sample length, 40 cm, was first selected from the reservoir top. The correlation coefficients between the values of T_2 and ϕ_{NMR} located in the interval were then calculated, referred to as R_{corr}. In the next step, the interval was moved forward by the depth sampling rate, and R_{corr} was recalculated. This process continued until the interval reached the bottom of the reservoir.

Removing Shale Information

T_2 and ϕ_{NMR} were correlated negatively with GR. The scatter plot of ϕ_{NMR} and T_2 vs. GR indicates that ϕ_{NMR} and T_2 decreased linearly with increasing GR. Figure 4a and b, for example, depicts this behavior in reservoir B. Table 3 shows the values of R between ϕ_{NMR} and GR $\left(R_{\phi_{NMR},GR}\right)$ and

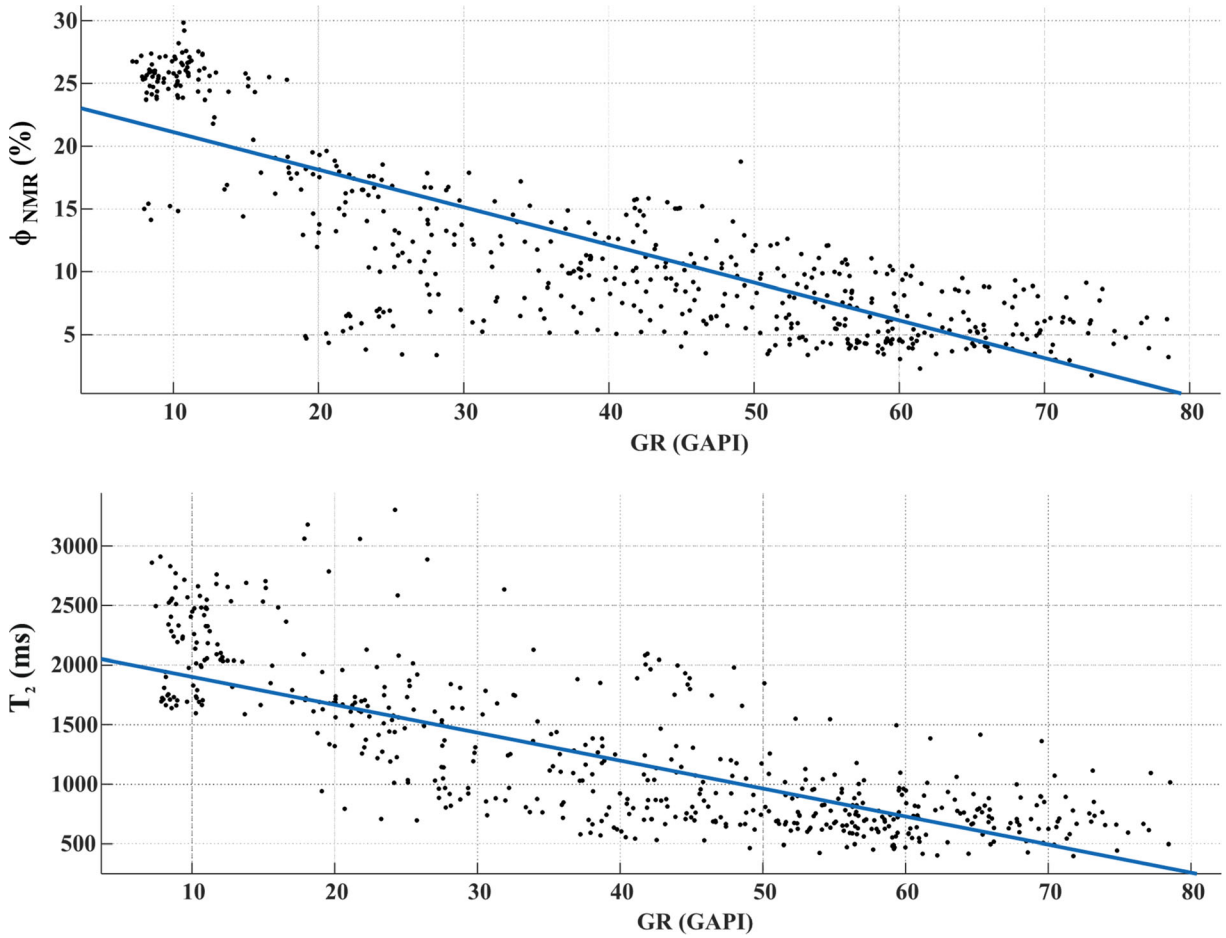

Figure 4. Increasing GR in reservoir B with linear decline of ϕ_{NMR} (top) and T_2 (bottom).

Table 3. Values of $R_{\phi_{\mathrm{NMR}},GR}$ and $R_{T_2,GR}$ in the target reservoirs

Reservoir	$R_{\phi_{\mathrm{NMR}},GR}$	$R_{T_2,GR}$
A	− 0.75	− 0.68
B	− 0.81	− 0.79

between T_2 and GR $\left(R_{T_2,GR}\right)$ in the target reservoirs.

In this study, wettability was assumed to be associated with variation in R_{corr}. The shale content, if any, was excluded from R_{corr} to obtain a pure correlation coefficient. Put differently, R_{corr} must be decorrelated with GR. The correlation coefficient between R_{corr} and GR was calculated using Eq. 2 for reservoirs A and B. The values of R for reservoirs A and B were − 0.32 and 0.07, respectively. The values

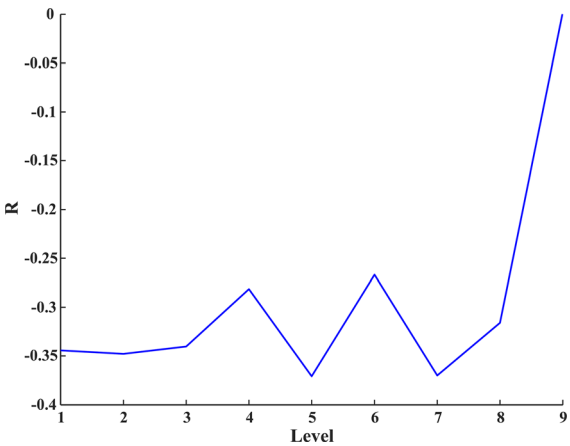

Figure 5. Values of R between the modified R_{corr} and GR vs. level in reservoir A.

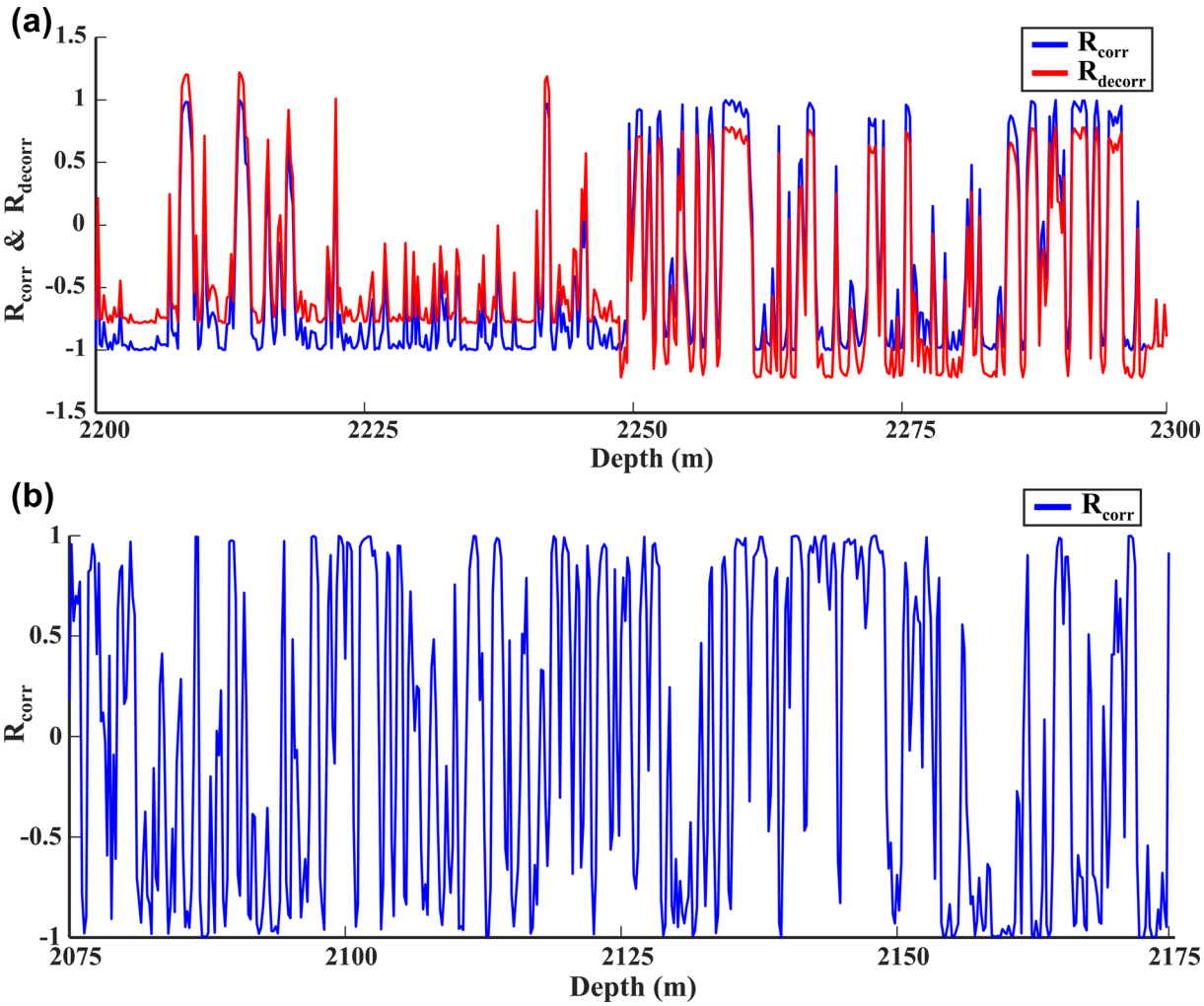

Figure 6. Values of R_{corr} and R_{decorr} vs. depth: **a** reservoir A; **b** reservoir B.

of $R \approx 0$ in reservoir B demonstrate that R_{corr} is uncorrelated with GR. Thus, removing the shale content from R_{corr} in reservoir A was essential to derive a pure correlation coefficient. The following steps were performed to remove the shale information from R_{corr}

1. The R_{corr} log was decomposed up to the maximum decomposition level (level 9). The detail coefficients at each level, $(D_1, D_2, \ldots, D_9)$, were extracted. $D_i(n) = (d_1, d_2 \ldots d_n)$ are the detail coefficients at level i, where $i = 1, \ldots, 9$.
2. The detail coefficients from levels 1 to 9, D_1 to D_9, were subtracted from the R_{corr} log, $(R_{\text{corr}} - D_1, R_{\text{corr}} - D_2, \ldots, R_{\text{corr}} - D_9)$. The resulting logs, $R_{\text{corr}} - D_{\text{i}}$, were referred to as the modified R_{corr} logs.
3. The correlation coefficient between each of the modified R_{corr} logs and GR log was calculated.

(4) The modified R_{corr} log resulting in a minimum value of R was selected and referred to as the decorrelated coefficient (R_{decorr}) log.

.

Figure 5 shows the values of R between the modified R_{corr} and GR vs. decomposition level. The value of R between the modified R_{corr} and GR becomes zero by removing D_9 from the R_{corr} log. Hence, the shale information is at level 9 of the R_{corr} log. Figure 6a and b demonstrates the values of R_{corr}

Table 4. Value of ΔR_{decorr} obtained from decomposing the R_{decorr} log with various wavelets

Depth	Daubechies (db1)	Symlet (sym4)	Coiflet (Coif1)	Reverse biorthogonal (rbio2.2)	Biorthogonal (bior2.2)
2212.8–2213.2	0.164	0.151	0.059	0.0427	0.029
2225.7–2226.1	− 0.0319	− 0.044	− 0.137	− 0.153	− 0.166
2227.6–2228.0	0.596	0.583	0.492	0.475	0.462
2232.2–2232.6	0.435	0.422	0.33	0.314	0.3
2234.3–2234.7	0.55	0.537	0.445	0.428	0.416
2238.3–2238.7	0.357	0.344	0.252	0.235	0.222
2241.0–2241.4	− 0.032	− 0.045	− 0.137	− 0.154	− 0.166
2241.5–2241.9	− 0.018	− 0.031	− 0.123	− 0.139	− 0.153
2242.3–2242.7	0.309	0.297	0.205	0.188	0.175
2247.6–2248.0	0.011	− 0.002	− 0.094	− 0.11	− 0.123
2249.5–2249.9	− 0.63	− 0.641	− 0.734	− 0.75	− 0.763
2264.0–2264.4	1.16	1.147	1.055	1.038	1.025
2266.0–2266.4	0.856	0.843	0.751	0.734	0.722
2269.5–2269.9	0.84	0.827	0.734	0.717	0.704

Table 5. Sum of absolute difference between ΔR_{decorr} and I_{W-O} for each discrete wavelet

Daubechies (db1)	Symlet (sym4)	Coiflet (Coif1)	Reverse biorthogonal (rbio2.2)	Biorthogonal (bior2.2)
2.308	2.157	1.266	1.247	1.264

and R_{decorr} vs. depth in reservoirs A and B, respectively.

Wettability in Reservoir A

The DWT was employed to extract the variations of R_{decorr} in reservoir A. To this end, the R_{decorr} log was decomposed to a level where coarse coefficients became equal. In this case, the R_{decorr} log is written as the sum of a decomposition constant $\left(R^{c}_{\text{decorr}}\right)$ and detail coefficients $(\Delta R_{\text{decorr}})$:

$$R_{\text{decorr}}(n) = R^{c}_{\text{decorr}} + \Delta R_{\text{decorr}}(n) \qquad (9)$$

$\Delta R_{\text{decorr}}(n)$ represents the variation in R_{decorr} at each depth. The value of ΔR_{decorr} is dependent on the type of discrete wavelet applied. Table 4 exhibits the ΔR_{decorr} value obtained from the decomposition of the R_{decorr} log with different discrete wavelets. The depth range of ΔR_{decorr} corresponds to that of the core sample. Table 5 shows the sum of the absolute difference between the corresponding ΔR_{decorr} and I_{W-O} values, $\sum|\Delta R_{\text{decorr}} - I_{W-O}|$, for each discrete wavelet. The rbio2.2 wavelet yielded the lowest value of $\sum|\Delta R_{\text{decorr}} - I_{W-O}|$. Accordingly, the ΔR_{decorr} values obtained from the decomposition of the R_{decorr} log with rbio2.2 closely matched the I_{W-O} values. The negative and positive values of ΔR_{decorr} correspond to oil-wet rock and water-wet rock, respectively. Figure 7 shows the plot of ΔR_{decorr} and I_{W-O} vs. core sample number. Figure 8 demonstrates the wettability $(\Delta R_{\text{decorr}})$ log. Figure 9 illustrates the distribution of ΔR_{decorr} values. According to the histogram, 60% of the ΔR_{decorr}

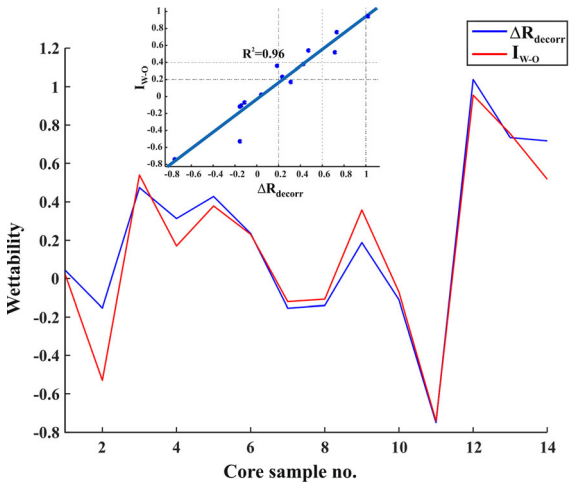

Figure 7. Reservoir A: plot of ΔR_{decorr} and I_{W-O} vs. core sample number. The superimposed image shows the linear relationship between ΔR_{decorr} and I_{W-O} with regression coefficient of 0.96.

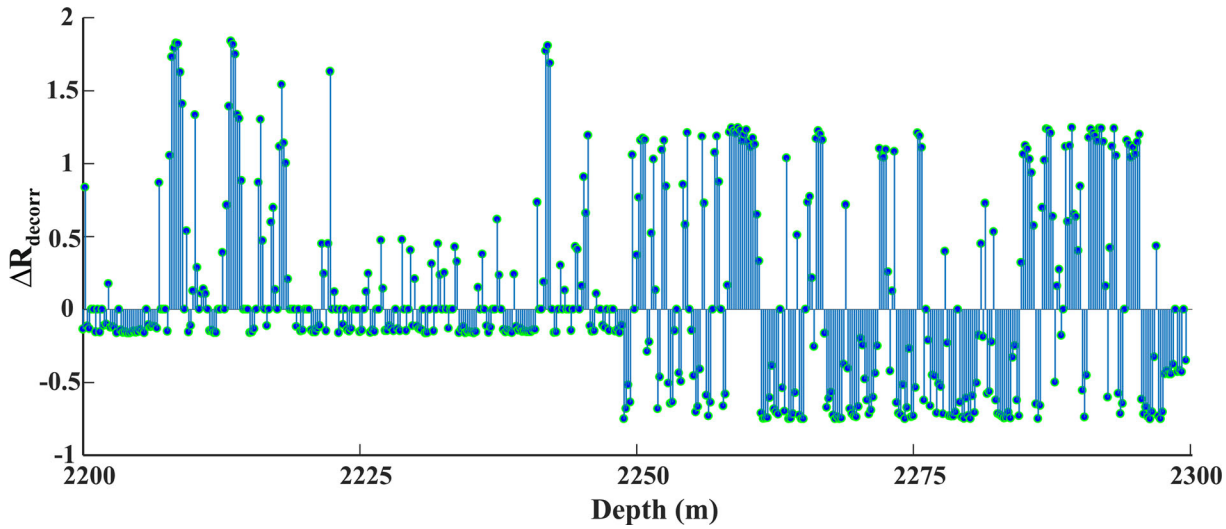

Figure 8. Reservoir A: wettability (ΔR_{decorr}) vs. depth.

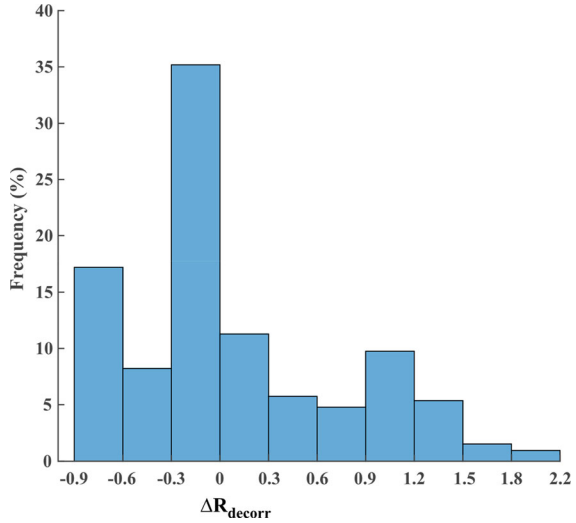

Figure 9. Reservoir A: distribution of ΔR_{decorr} values.

values were negative. Consequently, reservoir A is mainly oil-wet.

Wettability in Reservoir B

In reservoir B, R_{corr} was uncorrelated with GR. The DWT was used to decompose the R_{corr} log. A suitable wavelet was required to obtain the R_{corr} variations representing the reservoir rock wettability. There was a limited wettability test in this reservoir to ascertain the appropriate wavelet for extraction of the R_{corr} variations (ΔR_{corr}). Therefore, the intensity of wettability cannot be determined. The results obtained from the application of different discrete wavelets in reservoir A indicated that the ΔR_{decorr} sign did not change (Table 4). Accordingly, the type of wettability can be determined with any discrete wavelet. The rbio2.2 wavelet was chosen to extract ΔR_{corr} in reservoir B. Figure 10 demonstrates the ΔR_{corr} log. Figure 11 illustrates the distribution of ΔR_{corr} values. The percentage of negative values (53.15%) was slightly higher than that of positive values (46.85%). Accordingly, reservoir B is slightly oil-wet. This result was derived using the hypothetical rbio2.2 wavelet. By adopting the suitable wavelet, the correct range and frequency of ΔR_{corr} were obtained.

In this study, an interval equivalent to the length of the core sample was defined to calculate the R_{corr} value at each depth. The ΔR_{decorr} and ΔR_{corr} value vs. depth in reservoirs A and B indicated the in situ wettability, respectively. As the interval increased, ΔR_{decorr} (or ΔR_{corr}) represented the wettability in the larger depth range.

CONCLUSIONS

This research introduced a novel approach for characterizing the in situ wettability of two carbonate reservoirs based on NMR log data and wavelet transform. In this regard, the correlation coefficient

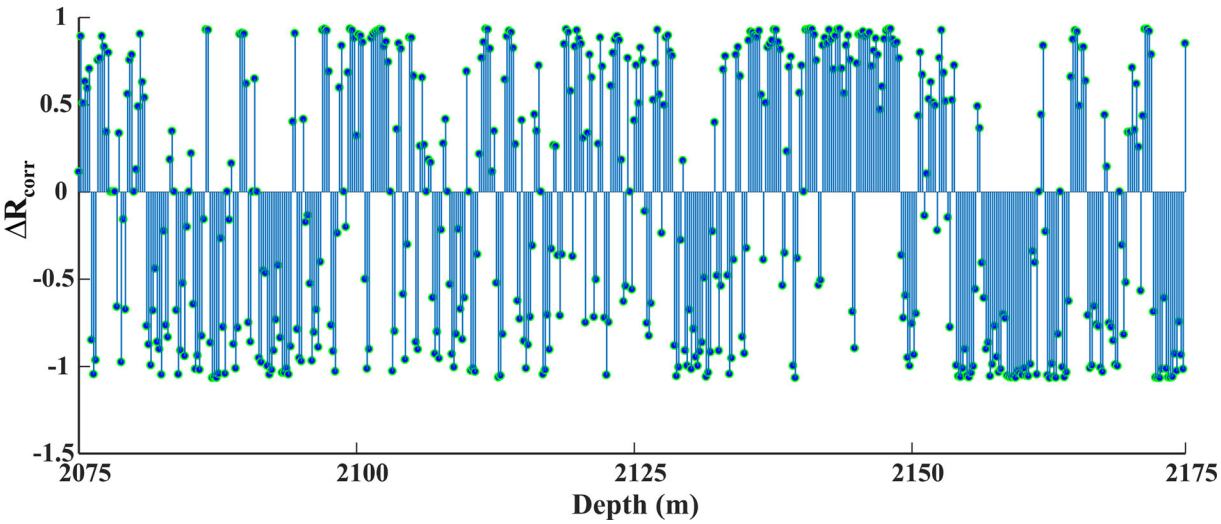

Figure 10. Reservoir B: wettability (ΔR_{corr}) vs. depth.

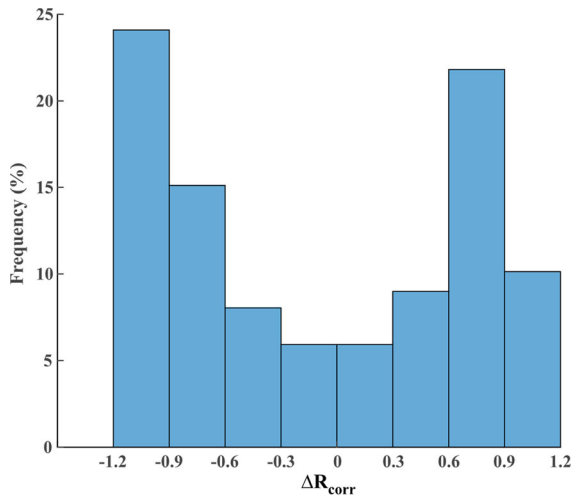

Figure 11. Reservoir B: distribution of ΔR_{corr} values.

between T_2 and ϕ_{NMR} was first calculated at each depth. The DWT was then applied to remove the shale content from the correlation coefficient log. The resulting log was referred to as the decorrelated coefficient log. Finally, the DWT was used to extract the detail coefficients from the decorrelated coefficient log. The detail coefficients were strictly consistent with the results of the wettability test. The main findings of this investigation were as follows.

1. The positive and negative detail coefficients obtained from decomposing the decorrelated coefficient log corresponded to water-wet and oil-wet rocks, respectively.
2. There is only a particular wavelet in each reservoir that can accurately yield the wettability log. A sufficient number of laboratory tests have to be implemented to ascertain such a wavelet.

REFERENCES

Al-Muthana, A., Hursan, G., Ma, S., Singer, P. M., Nicot, B., Valori, A., et al. (2016). Methods for determining wettability from NMR. Google Patents.

Awotunde, A. A., & Horne, R. N. (2013). Reservoir description with integrated multiwell data using two-dimensional wavelets. *Mathematical Geosciences, 45*(2), 225–252.

Azamipour, V., Misaghian, N., & Assareh, M. (2020). Multi-level optimization of reservoir scheduling using multi-resolution wavelet-based up-scaled models. *Natural Resources Research, 29*(3), 2103–2125.

Cheng, F., Yujiang, S., Jianfei, H., Zhenlin, W., Zhiqiang, M., Gaoren, L., et al. (2017). Nuclear magnetic resonance features of low-permeability reservoirs with complex wettability. *Petroleum Exploration and Development, 44*(2), 274–279.

Coates, G. R., Xiao, L., & Prammer, M. G. (1999). *NMR logging: Principles and applications*. Gulf Professional Publishing.

Dick, M., Veselinovic, D., & Green, D. (2019). Spatially resolved wettability measurements using nmr wettability index. In: *E3S Web of conferences, 2019* (Vol. 89, pp. 03001): EDP Sciences.

Dunn, K. J., Bergman, D. J., & LaTorraca, G. A. (2002). *Nuclear magnetic resonance: Petrophysical and logging applications* (Vol. 32): Elsevier.

Ge, X., Fan, Y., Li, J., Wang, Y., & Deng, S. (2015). Noise reduction of nuclear magnetic resonance (NMR) transversal data using improved wavelet transform and exponentially weighted moving average (EWMA). *Journal of Magnetic Resonance, 251,* 71–83.

Grasseau, N., Grélaud, C., López-Blanco, M., & Razin, P. (2019). Forward seismic modeling as a guide improving detailed seismic interpretation of deltaic systems: Example of the Eocene Sobrarbe delta outcrop (South-Pyrenean foreland basin, Spain), as a reference to the analogous subsurface Albian-Cenomanian Torok-Nanushuk Delta of the Colville Basin (NPRA, USA). *Marine and Petroleum Geology, 100,* 225–245.

Hayter, A. J. (2012). *Probability and statistics for engineers and scientists* (4 edn). Cengage Learning.

Heidary, M., & Fouladi Hossein Abad, K. (2020). A wavelet-based model for determining asphaltene onset pressure. *Natural Resources Research*. https://doi.org/10.1007/s11053-020-09753-w.

Heidary, M., Kazemzadeh, E., Moradzadeh, A., & Bagheri, A. M. (2019). Improved identification of pay zones in complex environments through wavelet analysis on nuclear magnetic resonance log data. *Journal of Petroleum Science and Engineering, 172,* 465–476.

Jansen, M. H., & Oonincx, P. J. (2005). *Second generation wavelets and applications*. Springer Science & Business Media.

Katika, K., Saidian, M., & Fabricius, I. L. (2016). Wettability of chalk and argillaceous sandstones assessed from T1/T2 ratio. In: *78th EAGE conference and exhibition 2016, 2016*.

Korb, J.-P., Nicot, B., & Jolivet, I. (2018). Dynamics and wettability of petroleum fluids in shale oil probed by 2D T1–T2 and fast field cycling NMR relaxation. *Microporous and Mesoporous Materials, 269,* 7–11.

Liang, C., Xiao, L., Zhou, C., Wang, H., Hu, F., Liao, G., et al. (2019a). Wettability characterization of low-permeability reservoirs using nuclear magnetic resonance: An experimental study. *Journal of Petroleum Science and Engineering*.

Liang, C., Xiao, L., Zhou, C., Zhang, Y., Liao, G., & Jia, Z. (2019b). Two-dimensional nuclear magnetic resonance method for wettability determination of tight sand. *Magnetic Resonance Imaging, 56,* 144–150.

Looyestijn, W. J., & Hofman, J. (2006). Wettability-index determination by nuclear magnetic resonance. *SPE Reservoir Evaluation and Engineering, 9*(02), 146–153.

Minh, C. C., Crary, S., Singer, P. M., Valori, A., Bachman, N., Hursan, G., et al. Determination of wettability from magnetic resonance relaxation and diffusion measurements on fresh-state cores. In: *SPWLA 56th annual logging symposium, 2015*: Society of Petrophysicists and Well-Log Analysts.

Rezapour, A., Ortega, A., & Sahimi, M. (2019). Upscaling of geological models of oil reservoirs with unstructured grids using lifting-based graph wavelet transforms. *Transport in Porous Media, 127*(3), 661–684.

Saadatinejad, M. R., & Sarkarinejad, K. (2011). Application of the spectral decomposition technique for characterizing reservoir extensional system in the Abadan Plain, southwestern Iran. *Marine and Petroleum Geology, 28*(6), 1205–1217.

Sauerer, B., Valori, A., Krinis, D., & Abdallah, W. (2019). NMR wettability of carbonate reservoir cores: best practices. In: *SPE middle east oil and gas show and conference, 2019*. Society of Petroleum Engineers.

Valori, A., Hursan, G., & Ma, S. M. (2017). Laboratory and downhole wettability from NMR T 1/T 2 ratio. *Petrophysics, 58*(04), 352–365.

Wang, J., Xiao, L., Liao, G., Zhang, Y., Cui, Y., Sun, Z., et al. (2019). NMR characterizing mixed wettability under intermediate-wet condition. *Magnetic Resonance Imaging, 56,* 156–160.

Wu, Y. B., Xie, R. H., & Xiao, L. Z. (2012). Application of wavelet domain adaptive filtering to de-noise NMR Data. In: *Advanced materials research, 2012* (Vol. 588, pp. 814–817). Trans Tech Publ.

Xie, R., Wu, Y., Liu, K., Liu, M., & Xiao, L. (2014). De-noising methods for NMR logging echo signals based on wavelet transform. *Journal of Geophysics and Engineering, 11*(3), 035003.

Xu, H., & Sun, S. Z. (2014). Seismic singularity attribute and its applications in sub-seismic faults detection. *Acta Geodaetica et Geophysica, 49*(4), 403–414.

Yue, D., Li, W., Wang, W., Hu, G., Qiao, H., Hu, J., et al. (2019). Fused spectral-decomposition seismic attributes and forward seismic modelling to predict sand bodies in meandering fluvial reservoirs. *Marine and Petroleum Geology, 99,* 27–44.